

Transverse modes of a cigar-shaped Bose-Einstein condensate

B. Jackson and E. Zaremba

Department of Physics, Queen's University, Kingston, Ontario K7L 3N6, Canada

brian@sparky.phy.queensu.ca

(November 20, 2018)

Abstract

We discuss the collective modes in a harmonically trapped, highly-elongated Bose condensed gas. The transverse breathing mode exhibits a number of interesting features, such as the insensitivity of the condensate mode frequency to the interaction strength, and the closeness of the frequency to that of the non-condensed thermal cloud in the collisionless limit. Using finite temperature simulations, we show that these features are responsible for the very small damping rate observed experimentally. Our results for the temperature dependence of the damping rate and frequency shift are in excellent agreement with experiment. We also demonstrate that the unusually small damping rate does not arise for the $m = 2$ mode or for more isotropic trap potentials, suggesting further possible experimental tests of our theory.

PACS numbers: 03.75.Fi, 05.30.Jp, 67.40.Db

arXiv:cond-mat/0208567v1 [cond-mat.stat-mech] 28 Aug 2002

I. INTRODUCTION

The study of the finite temperature properties of trapped Bose-Einstein condensed gases touches on fundamental issues such as condensate growth and relaxation processes in an isolated quantum degenerate system. As such, they have been the subject of ongoing research since soon after the Nobel prize-winning discoveries of 1995. For example, early experiments at JILA [1] and MIT [2] measured the frequency and damping rates of collective excitations as a function of temperature. More recent experiments have studied the finite temperature behavior of the scissors mode [3], and the radial breathing mode in a cigar-shaped condensate [4]. These experiments have in turn stimulated a considerable amount of theoretical work.

Finite temperature theories have taken various forms. Early work focussed on solving Hartree-Fock-Bogoliubov (HFB) equations to find the excitation spectrum of the system [5–7]. These excited states, when thermally occupied, determine the equilibrium density distribution of the non-condensed thermal cloud. Unfortunately, this method is unsatisfactory when considering the low energy collective modes since it treats the thermal cloud as static. In reality the condensate oscillations will induce fluctuations in the thermal component, which then act back on the condensate leading to damping and associated frequency shifts. One possible way of addressing this problem is to treat the thermal cloud dynamics perturbatively. This method has been pursued by a number of authors [8–12], and although good agreement has been found with some of the experimental results [1,2], it is still unclear whether the method is useful in situations where the full dynamics of the thermal cloud is important.

An alternative approach is to formulate a quantum kinetic theory, which in principle treats the dynamics of the system fully and consistently. This includes second-order collisional processes, which lead to equilibration of the system. Kinetic theories for dilute Bose gases have been formulated by Stoof [13], Gardiner and co-workers [14], Walser *et al.*, [15] and Zaremba, Nikuni and Griffin (ZNG) [16]. Finally, there is the possibility of treating the evolution of the system using Fokker-Planck equations for quasiprobability distributions. A specific example of this is the truncated Wigner representation, or classical field method [17,18], which is valid when the occupation of the relevant states is much greater than unity.

In this paper we shall present results of solving the ZNG equations using a method detailed in a previous publication [19]. Earlier applications of the method yielded results in good agreement with the scissors mode experiment at Oxford [3,20] as well as with the quadrupole modes in the JILA experiment [1,21]. Here we focus instead on the ENS experiment [4], adding more details to the discussion of our simulations in Ref. [22]. The ENS experiment studied the radial breathing mode of an elongated condensate, and found unusually small damping rates and frequency shifts as compared to other experiments. We explain this behaviour in terms of an accidental degeneracy between the condensate and thermal cloud oscillation frequencies. In Section II we review the ZNG theory and our numerical scheme, while in Section III we discuss the collective modes in an elongated harmonic trap. In Section IV we present results from our finite temperature simulations for the transverse breathing and quadrupole modes in this geometry. For the latter, the condensate and thermal cloud frequencies are no longer degenerate and we find a much larger damping rate and frequency shift. We also show that larger damping rates arise when the degeneracy is lifted in more isotropic trap potentials. Finally, Section V presents our

conclusions.

II. ZNG THEORY

We first give an overview of the ZNG theory which forms the basis of the numerical simulations described in this paper. Further details of the formalism, including the approximations made, can be found in Ref. [16]. In the theory two coupled equations are used to describe the condensate and thermal cloud dynamics. In particular, the condensate wavefunction $\Phi(\mathbf{r}, t)$ evolves according to the generalized Gross-Pitaevskii (GP) equation

$$i\hbar\frac{\partial}{\partial t}\Phi(\mathbf{r}, t) = \left(-\frac{\hbar^2\nabla^2}{2m} + U_{\text{ext}}(\mathbf{r}, t) + g[n_c(\mathbf{r}, t) + 2\tilde{n}(\mathbf{r}, t)] - iR(\mathbf{r}, t)\right)\Phi(\mathbf{r}, t). \quad (1)$$

The condensate interacts locally with other condensate atoms and with the non-condensate, with interactions parametrized by $g = 4\pi\hbar^2 a/m$, where a is the s -wave scattering length and m is the mass of the atoms. These mean-field interactions involve the condensate density $n_c(\mathbf{r}, t) = |\Phi(\mathbf{r}, t)|^2$ and the non-condensate density $\tilde{n}(\mathbf{r}, t)$. The term $U_{\text{ext}}(\mathbf{r}, t) = m[\omega_\perp^2(x^2 + y^2) + \omega_z^2 z^2]/2$ represents the trap potential. The frequencies in the radial (ω_\perp) and axial (ω_z) directions are generally different, and the ratio $\lambda = \omega_z/\omega_\perp$ conveniently parameterizes the trap anisotropy.

The thermal cloud is described in terms of a semiclassical Wigner distribution $f(\mathbf{p}, \mathbf{r}, t)$ which defines the non-condensate density according to

$$\tilde{n}(\mathbf{r}, t) = \int \frac{d\mathbf{p}}{(2\pi\hbar)^3} f(\mathbf{p}, \mathbf{r}, t). \quad (2)$$

This distribution function satisfies the kinetic equation

$$\frac{\partial}{\partial t}f(\mathbf{p}, \mathbf{r}, t) + \frac{\mathbf{p}}{m} \cdot \nabla f(\mathbf{p}, \mathbf{r}, t) - \nabla U(\mathbf{r}, t) \cdot \nabla_{\mathbf{p}} f(\mathbf{p}, \mathbf{r}, t) = C_{12}[f] + C_{22}[f], \quad (3)$$

where the term $U(\mathbf{r}, t) = U_{\text{ext}}(\mathbf{r}) + 2g[n_c(\mathbf{r}, t) + \tilde{n}(\mathbf{r}, t)]$ reflects the combined effect of the trap and mean-field potentials on the thermal cloud evolution. Interactions also enter in the terms on the right-hand side, which are of order g^2 and correspond to binary collision events between thermal atoms (C_{22}) and between thermal and condensate atoms (C_{12}). The second process is particularly important in the context of condensate growth, since it leads to a transfer of atoms between the condensate and thermal cloud. It also accounts for the non-Hermitian term in the GP equation (1) which is given by

$$R(\mathbf{r}, t) = \frac{\hbar}{2n_c} \int \frac{d\mathbf{p}}{(2\pi\hbar)^3} C_{12}[f]. \quad (4)$$

This term has the effect of changing the normalization of the condensate wavefunction.

We note that the kinetic equation (3) for the thermal excitations is the same as that for gas of classical particles moving in the effective potential U . This is the basis of our numerical solution of this equation, which tracks the Hamiltonian dynamics of a swarm of test particles using a symplectic integrator. Collisions are treated using a Monte Carlo evaluation of the collision integrals. The GP equation can be propagated in time using a variety of methods, but we favour a Fast Fourier Transform split-step operator technique. More details of the numerical methods can be found in Ref. [19].

III. COLLECTIVE MODES

In this section we discuss the collective modes of the system, with particular emphasis on the so-called transverse breathing mode in a cigar-shaped trap. We begin by reviewing results for a pure condensate at temperature $T = 0$. In this limit the condensate dynamics is described by (1) with $\tilde{n} = 0$ and $R = 0$, i.e.,

$$i\hbar\frac{\partial}{\partial t}\Phi(\mathbf{r}, t) = \left(-\frac{\hbar^2\nabla^2}{2m} + U_{\text{ext}}(\mathbf{r}) + gn_c(\mathbf{r}, t)\right)\Phi(\mathbf{r}, t). \quad (5)$$

The equilibrium solution can be found from (5) by making the substitution $\Phi(\mathbf{r}, t) = \Phi_0(\mathbf{r})e^{-i\mu t}$, where μ is the chemical potential. When the number of atoms is sufficiently large, the kinetic energy term is dominated by the other terms and can be neglected. This defines the Thomas-Fermi (TF) approximation and gives an equilibrium density profile of

$$n_{c0}(\mathbf{r}) = \frac{1}{g}[\mu - U_{\text{ext}}(\mathbf{r})]. \quad (6)$$

The frequencies of condensate excitations can be found by linearizing (5), and analytic solutions for the lowest modes in the TF limit were first presented by Stringari [23]. In a spherical trap ($\lambda = 1$), the modes can be labelled by the angular momentum quantum numbers (l, m) . The lowest of these modes correspond to monopole $(0, 0)$ and quadrupole $(2, 0)$ excitations with frequencies $\sqrt{5}\omega_{\perp}$ and $\sqrt{2}\omega_{\perp}$, respectively. In an anisotropic, axisymmetric trap these two modes are coupled to give the dispersion relation

$$\omega_{\pm}^2 = \omega_{\perp}^2 \left(2 + \frac{3}{2}\lambda^2 \pm \frac{1}{2}\sqrt{9\lambda^4 - 16\lambda^2 + 16}\right). \quad (7)$$

In Fig. 1 we plot these two solutions as a function of λ . The two curves tend to the monopole and quadrupole frequencies of the isotropic trap in the $\lambda \rightarrow 1$ limit. For the cigar-shaped condensate which will be of interest here ($\lambda \ll 1$), the low frequency mode ω_{-} corresponds to a breathing-like oscillation predominately along the axial (z) direction, while the high-lying mode ω_{+} is associated with the radial breathing mode. In the limit $\lambda \rightarrow 0$ the frequency of the latter approaches $2\omega_{\perp}$. For example, in the experiment of Ref. [4], $\lambda \simeq 6.46 \times 10^{-2}$ and the transverse breathing mode has a frequency of $\omega_{+} \simeq 2.00052\omega_{\perp}$.

These results are valid in the strongly interacting TF regime, but the non-interacting limit $g = 0$ is also instructive. In this case the transverse quadrupole and breathing modes mentioned above both have a frequency of $2\omega_{\perp}$. This clearly has interesting consequences for the breathing mode in the $\lambda = 0$ limit, since it implies that the frequency is the same in the non-interacting and strongly-interacting limits. Indeed, calculations confirm [24] that this is also true in the intermediate regime, demonstrating the unusual property that the frequency of this mode is independent of interactions. This behavior is reminiscent of that for a gas in a 2D harmonic trap interacting by means of a contact potential [25,26], where there exists an undamped breathing mode with frequency $2\omega_{\perp}$, independent of interaction strength, temperature, or statistics.

The thermal cloud dynamics above T_c is given by (3) with $n_c = 0$ and $C_{12} = 0$, i.e.,

$$\frac{\partial}{\partial t}f(\mathbf{p}, \mathbf{r}, t) + \frac{\mathbf{p}}{m} \cdot \nabla f(\mathbf{p}, \mathbf{r}, t) - \nabla U_{\text{ext}}(\mathbf{r}, t) \cdot \nabla_{\mathbf{p}}f(\mathbf{p}, \mathbf{r}, t) = C_{22}[f], \quad (8)$$

where for simplicity we have also neglected the thermal cloud mean field term, $2g\tilde{n}$, since it has a very small effect on the dynamics in the normal state. The lowest collective modes for the thermal gas can be conveniently found from (8) by taking moments. This procedure was used to study a classical gas in [27], though the results for a non-condensed Bose gas are essentially the same. The frequency and damping of the modes depend upon the mean collision rate τ^{-1} relative to the frequency of the mode ω . In the purely collisionless regime $\omega\tau \rightarrow \infty$, and the frequencies of the transverse quadrupole and breathing modes are both $\omega = 2\omega_{\perp}$, while the damping is zero. In the hydrodynamic limit ($\omega\tau \rightarrow 0$) the modes are also undamped, but here the frequencies of the respective modes are $\omega_Q = \sqrt{2}\omega_{\perp}$ and $\omega_M = \sqrt{10/3}\omega_{\perp}$ (where the latter is specifically for the cigar-shaped limit $\lambda \ll 1$) [27,28]. In general the modes will be damped through collisions, and will have a frequency intermediate between these two limits. In the experiment of [4] the system resided in the near-collisionless regime, so that both thermal cloud modes were only weakly damped with frequency $\omega \simeq 2\omega_{\perp}$.

In order to understand the transverse breathing mode more fully it is instructive to derive an equation of motion for the operator $R^2 = \sum_i (x_i^2 + y_i^2)$. The expectation value of this operator for a particular dynamical state gives the mean-squared radial size of the cloud and it is therefore a suitable variable to describe the transverse breathing mode of interest. For the Hamiltonian

$$H = \sum_i \frac{p_i^2}{2m} + \frac{m}{2} \sum_i [\omega_{\perp}^2 (x_i^2 + y_i^2) + \omega_z^2 z_i^2] + \frac{g}{2} \sum_{i \neq j} \delta(\mathbf{r}_i - \mathbf{r}_j), \quad (9)$$

we have the Heisenberg equation of motion

$$\frac{dR^2}{dt} = \frac{i}{\hbar} [H, R^2] = \frac{Q}{m}, \quad (10)$$

where the operator Q is given by

$$Q = \sum_i (x_i p_{ix} + y_i p_{iy} + \text{h.c.}). \quad (11)$$

After differentiating (10) again and evaluating the commutator $[H, Q]$ we obtain the result

$$\frac{d^2 R^2}{dt^2} + (2\omega_{\perp})^2 R^2 = \frac{4}{m} (H - T_z - U_z^{\text{ext}}), \quad (12)$$

where $T_z = \sum_i (p_{iz}^2/2m)$ is the kinetic energy associated with motion in the z -direction and $U_z^{\text{ext}} = \sum_i (m\omega_z^2 z_i^2/2)$. It is worth emphasizing that this equation for R^2 is an operator identity which is equally valid classically as it is quantum mechanically.

We now consider the expectation value of (12) with respect to some nonequilibrium density matrix. Denoting expectation values by angular brackets, and noting that the energy, E , of the system is a constant of the motion, we have

$$\frac{d^2 \chi}{dt^2} + (2\omega_{\perp})^2 \chi = \frac{4}{m} [E - \langle T_z \rangle - \langle U_z^{\text{ext}} \rangle], \quad (13)$$

where we have defined $\chi \equiv \langle R^2 \rangle$. For a strictly two-dimensional (2D) system, $\langle T_z \rangle = \langle U_z^{\text{ext}} \rangle = 0$, and (13) has the solution

$$\chi = A \cos(2\omega_{\perp}t) + \bar{\chi}. \quad (14)$$

In other words, χ oscillates about $\bar{\chi} = E/(m\omega_{\perp}^2)$ with frequency $2\omega_{\perp}$. This behaviour was first noted by Pitaevskii and Rosch in their analysis of the 2D system. For three-dimensional systems, $\langle T_z \rangle$ and $\langle U_z^{\text{ext}} \rangle$ are themselves dynamical variables. Their appearance in (13) will in general lead to a shift of the frequency of the transverse breathing mode from $2\omega_{\perp}$, except in certain limiting cases.

The equation of motion for mean values in (13) is also valid when the dynamics is governed by the time-dependent GP equation. However in this case, the average of an operator \mathcal{O} is defined as $\langle \mathcal{O} \rangle = \int d\mathbf{r} \Phi^*(\mathbf{r}, t) \mathcal{O} \Phi(\mathbf{r}, t)$. In the limit of a cylindrical trap, $\lambda \rightarrow 0$ and $\langle U_z^{\text{ext}} \rangle = 0$. If we then consider an axially symmetric mode which is spatially invariant along the length of the trap, we have $\langle T_z \rangle = 0$ and (13) implies that a mode at the frequency $2\omega_{\perp}$ exists. This particular mode was previously identified as the transverse breathing mode in a cylindrical trap. It should be emphasized that this conclusion is based on the approximate GP description. In the many-body treatment, $\langle T_z \rangle \neq 0$ and the existence of a $2\omega_{\perp}$ mode then depends on $\langle T_z \rangle$ being constant. It is not known whether a dynamical state with this property exists in general.

In applying (13) to a semiclassical gas we interpret the expectation value of a physical observable \mathcal{O} as the phase space average $\langle \mathcal{O} \rangle = \int (d\mathbf{p}d\mathbf{r}/h^3) \mathcal{O}(\mathbf{p}, \mathbf{r}) f(\mathbf{p}, \mathbf{r}, t)$. Two limits are of interest: the collisionless and the hydrodynamic. In the former case one can use (8) to show that $d(\langle T_z \rangle + \langle U_z^{\text{ext}} \rangle)/dt = 0$ for a separable confining potential. Eq. (13) then implies that a collisionless gas has a transverse breathing mode at the frequency $2\omega_{\perp}$, as noted earlier.

Once collisions are included, $(\langle T_z \rangle + \langle U_z^{\text{ext}} \rangle)$ is no longer a constant of the motion and the frequency of the transverse breathing mode will change. We can illustrate this for a cylindrical trap ($\omega_z = 0$) in the hydrodynamic limit. In this regime, collisions are sufficiently frequent to ensure local thermodynamic equilibrium, so that the distribution function is of the Bose form

$$f(\mathbf{p}, \mathbf{r}, t) = \frac{1}{e^{\beta(\mathbf{r}, t) \{[\mathbf{p} - m\mathbf{v}(\mathbf{r}, t)]^2/2m - \mu(\mathbf{r}, t)\} - 1}}, \quad (15)$$

where $\beta(\mathbf{r}, t)$, $\mu(\mathbf{r}, t)$ and $\mathbf{v}(\mathbf{r}, t)$ are all local hydrodynamic variables. For the transverse breathing mode the local velocity field has the form $\mathbf{v}(\mathbf{r}, t) = a\mathbf{r}_{\perp}$, where \mathbf{r}_{\perp} is a vector in the radial direction, transverse to the axis of the trap. Using (15) one can show that $\langle T_z \rangle = \langle T \rangle/3$ and $E = \langle T \rangle + m\omega_{\perp}^2 \chi/2$, where we have neglected the nonlinear contribution of the velocity field to the kinetic energy $\langle T \rangle = \langle p^2/2m \rangle$ of the mode. By substituting these expressions into (13) one finds that the transverse breathing mode has frequency $\omega_M = \sqrt{10/3}\omega_{\perp}$, in agreement with other calculations in this limit [27,28]. This provides a concrete example of a situation in which a non-constant $\langle T_z \rangle$ leads to a shift in the mode frequency from $2\omega_{\perp}$. It is therefore clear that a mode at this frequency is not a universal property of a trapped gas in the cylindrical geometry.

IV. NUMERICAL RESULTS

The behavior of the condensate at $0 < T < T_c$ is influenced by the presence of thermal excitations. Normally this leads to a decay of condensate oscillations, which in the near-

collisionless regime arises through Landau damping. There is also an associated frequency shift. However, in the experiment of [4], the transverse breathing mode was found to be very weakly damped, with a frequency almost independent of temperature. This is in stark contrast to the much larger damping rate found in their measurements of the quadrupole mode, as well as in other experiments [1–3]. In this section we present results of both the breathing and quadrupole modes for the system studied in Ref. [4]. We show that the observed behavior of the breathing mode is a consequence of the degeneracy of the condensate and thermal cloud mode frequencies coupled with the fact that both components are initially excited.

The experimental scheme used to excite the system was to suddenly change the radial trap frequency and then to reset it to its original value after some short time τ . This stepped excitation can be represented by

$$\omega'_{\perp}(t) = \omega\{1 + \alpha[\Theta(t) - \Theta(t - \tau)]\}, \quad (16)$$

where we take $\omega_{\perp} = 2\pi \times 182.6$ Hz, $\alpha = 0.26$, and $\omega_{\perp}\tau = 0.172$. Although this is a relatively simple method for exciting condensate oscillations, in finite temperature studies it has the disadvantage of also exciting the thermal cloud. This aspect is relatively unimportant when the oscillation frequencies of the condensate and thermal cloud are sufficiently different, but when they are similar it can have a profound effect on the behavior of the system. An important implication is that the usual perturbative calculation of Landau damping which assumes the thermal cloud to be at rest [8–12] are no longer applicable.

To illustrate this point, we show in Fig. 2(a) the result of a simulation at $T = 125$ nK (as compared to the experimentally measured critical temperature of $T_c \simeq 290$ nK). We plot the radial moments for the condensate, χ_c , and thermal cloud, χ_n , as a function of time, where each has been divided by its initial value to give the relative oscillation amplitude. One sees that both components respond to the stepped excitation by oscillating in phase with approximately equal amplitudes. In addition, the oscillation frequency is very close to $2\omega_{\perp}$ and the damping rate is very small. As discussed earlier, the frequency is that expected for the condensate for $\lambda \simeq 0$ and for the thermal cloud in the collisionless regime. The common in-phase oscillation of the two components is further reinforced by mean-field interactions. The lack of relative motion between the two components accounts for the fact that Landau damping is not effective. Evidence supporting this interpretation is provided in Fig. 2(b), where we plot the result of exciting only the condensate by imposing a radial velocity field, $\mathbf{v}_c \propto x\hat{\mathbf{i}} + y\hat{\mathbf{j}}$. In this case the condensate oscillates initially in the presence of a *stationary* thermal cloud and as a result, Landau damping is fully active, giving rise to the much larger damping rate seen here.

To quantify the frequency and damping rate, we fit the condensate oscillation to an exponentially decaying sinusoid $A \cos(\omega t + \varphi)e^{-\Gamma t} + C$. Fig. 3 compares our results at different temperatures with the experimental data. We see very good agreement between simulations and experiment for both the frequency and damping rate. As discussed in [22], the damping that occurs is essentially due to C_{12} and C_{22} collisional processes. This is unlike the situation for other modes in the near-collisionless regime [19,20] where in fact Landau damping is the dominant damping mechanism. As indicated in Fig. 2(b), Landau damping of the breathing mode only appears when the two components are moving relative to each other.

Recently, results from a calculation by Guilleumas and Pitaevskii appeared [29] that point to a different conclusion. They performed a perturbation theory calculation similar to [11], but for a cylindrically trapped condensate. In this geometry the excitation spectrum, as obtained from the Bogoliubov equations, is characterized by a series of curves continuous in k , the axial wavevector, with each curve corresponding to distinct radial (n) and azimuthal angular momentum (m) quantum numbers [30]. Calculation of the Landau damping rate then consists of evaluating the following expression

$$\Gamma = \frac{\pi}{\hbar^2} \sum_{ij} |A_{ij}|^2 (f_i - f_j) \delta(\omega_j - \omega_i - \omega_{osc}), \quad (17)$$

where the delta function reflects energy conservation of the decay process, in which a quantum of oscillation $\hbar\omega_{osc}$ is annihilated, and the i -th excitation transformed into the j -th. The probability of this transition is determined by the matrix element A_{ij} (as defined in Ref. [29]), and the distribution function f . The thermal cloud is assumed to be in thermodynamic equilibrium, so that the states i, j are thermally occupied according to the Bose distribution $f_i = [\exp(\hbar\omega_i/k_B T) - 1]^{-1}$. Using this method they calculated damping rates for the lowest $m = 0$ and $m = 2$ modes in the $k = 0$ limit, which corresponds to the transverse modes in the elongated 3D geometry. We shall discuss the $m = 2$ results later, but it is interesting that they found a damping rate for the $m = 0$ which is an order of magnitude *smaller* than the experimentally measured value. Since this calculation assumes a stationary thermal cloud, it is in fact *two* orders of magnitude smaller than our result for the analogous situation where only the condensate is excited initially [Fig. 2(b)].

The discrepancy between the two results could arise for a variety of reasons. It may be that the semiclassical approximation, as employed in our calculations, is not valid for this particular case. The small damping rate in Ref. [29] is partly the result of the small number of transitions that satisfy energy conservation. This constraint is less severe in the semiclassical approximation in which the excitations are continuous in *both* the axial and radial directions. The damping rate seen in [Fig. 2(b)] might therefore be an overestimate. On the other hand, there is also the possibility that the small damping rate is an artifact of the calculational method employed for the infinite cylinder. In the spherical trap discussed by the same authors [11], energy can never be conserved precisely in a transition due to the discreteness of the energy levels. So in practice the Landau damping rate (17) is calculated by replacing the delta functions with Lorentzians of finite width. In a previous publication [19] we found good agreement between this approach and our simulations. This procedure would have to be employed for any 3D system with a finite value of ω_z . Since the excitation spectrum is a continuous function of k for an infinite cylinder, this procedure for dealing with discrete excitations is not required. The neglect of off-energy shell transitions in this case may be leading to an underestimate of the damping rate as compared to the finite trap situation. In order to address these questions it would be useful to extend the perturbative calculations of [11] to elongated condensates. One could then study the variation of the damping with anisotropy to see whether the results begin to diverge from the semiclassical simulations at some point. We are currently exploring this possibility.

As we discussed above, the small damping rates and frequency shifts shown in Fig. 3 are a consequence of the fact that there is no relative motion of the condensate and thermal cloud in the transverse breathing mode. This behaviour does not occur if the two components

tend to oscillate at different frequencies as is the case for the $m = 2$ transverse quadrupole mode. To demonstrate this we have performed simulations for the $m = 2$ mode by imposing identical velocity fields of the form $\mathbf{v}_{\{c,n\}} \propto x\hat{\mathbf{i}} - y\hat{\mathbf{j}}$ on the two components. An example of the subsequent oscillations of the condensate and thermal cloud is shown in Fig. 4. One sees that the frequencies are indeed quite different in this case – the condensate oscillates with a frequency approximately equal to $\sqrt{2}\omega_{\perp}$, while the thermal cloud oscillates at a frequency close to $2\omega_{\perp}$. As for the $m = 0$ mode, we fit the condensate data to a damped sinusoid, and plot the frequency and damping rate as a function of temperature in Fig. 5. In contrast to the $m = 0$ data in Fig. 3, the $m = 2$ mode shows a much larger shift in frequency, as well as an order of magnitude increase in damping rate. The relative motion between the condensate and thermal cloud in this case accounts for these increases. Indeed, from the perspective of the condensate, the thermal cloud motion averages over the course of the simulation to that of a stationary cloud. This is confirmed by simulations where the thermal cloud is not excited initially. As seen in Fig. 5, these simulations exhibit very similar results to when both components are perturbed, especially when $T \leq 150$ nK. The differences between the two schemes at higher temperatures mainly reflect statistical variations of the results from one simulation to the next.

Interestingly, when Guilleumas and Pitaevskii [29] investigated the $m = 2$ mode for the cylindrical limit, they found damping rates in line with our results in Fig. 5, especially at higher temperatures. There are some discrepancies at low temperatures, but it must be remembered that precise agreement would not be expected between the two calculations due to differences in geometry, parameters and calculational method. Nonetheless, it is intriguing that such good agreement should be found here and not for the $m = 0$ mode. Again, further study is needed. Experiments for the $m = 2$ mode would also be of interest, since comparison to the results in Fig. 5 would provide further information regarding the reliability of our theory.

Finally, we discuss another method for breaking the degeneracy of the condensate and thermal cloud modes. As seen in Fig. 1, increasing the parameter λ leads to a rise in the breathing mode frequency ω_{+} , while at the same time the thermal cloud frequency remains near $2\omega_{\perp}$. Thus, as the trap becomes more isotropic the condensate frequency moves away from degeneracy, and one would expect the damping of the breathing mode to correspondingly increase. To check this we have performed simulations for larger values of λ . An example of the response to a stepped excitation (16) is shown in Fig. 6 for $\lambda = 0.75$; the geometric mean of the trap frequency is chosen to be the same as in the ENS experiment ($\bar{\omega} = \lambda^{1/3}\omega_{\perp} = 2\pi \times 73.3$ Hz). Fig. 6(b) shows the time dependence of the thermal cloud moment χ_n . It exhibits a damped oscillation at essentially one frequency; a single-mode fit to the data yielded a frequency of $\omega/\omega_{\perp} \simeq 2.007$ and a damping rate of $\Gamma/\omega_{\perp} \simeq 0.019$. The latter is approximately four times larger than found for the ENS geometry. The behavior of χ_c in Fig. 6(a) is more complex due to the fact that both of the ω_{\pm} modes are being excited. In fact, a combination of two damped sinusoids provided a very good fit to the time dependence shown and yielded the following fit parameters: $\omega_{-}/\omega_{\perp} \simeq 1.12$, $\Gamma_{-}/\omega_{\perp} \simeq 0.037$; $\omega_{+}/\omega_{\perp} \simeq 2.03$, $\Gamma_{+}/\omega_{\perp} \simeq 0.024$. The frequencies are quite close to the values given by (7) for $\lambda = 0.75$. More importantly, we see that the relative damping rate of the ω_{+} mode is approximately an order of magnitude larger than that of the transverse breathing mode from which it evolves. Thus even a relatively small difference in the frequencies of the condensate

and thermal cloud modes is sufficient to significantly enhance the Landau damping rate. This fact emphasizes the very special nature of the transverse breathing mode in the $\lambda \rightarrow 0$ limit.

V. SUMMARY

In this paper we have investigated the transverse oscillations of a Bose gas in the context of semiclassical finite temperature theory. Analytical results were derived in the cylindrical limit for the dynamics of the condensate at $T = 0$ and thermal cloud for $T > T_c$. Simulations are used to study the dynamics in an elongated trap at $0 < T < T_c$, for the parameters of the experiment of [4]. Our results for the frequency and damping of the $m = 0$ mode demonstrate very good agreement with this experiment. However, comparison to the results of a related theoretical study in [29] raises several interesting questions. We also study the $m = 2$ mode, and find a much larger damping rate and frequency shift associated with the presence in this case of relative motion between the condensate and thermal cloud. Finally, we study the effect on the $m = 0$ mode of decreasing the trap anisotropy, and find that the damping increases dramatically as soon as the accidental degeneracy between the condensate and thermal cloud frequencies is lifted.

ACKNOWLEDGMENTS

We acknowledge financial support from the Natural Sciences and Engineering Research Council of Canada, and the use of the HPCVL computing facilities at Queen's. We thank L. Pitaevskii for valuable discussions.

REFERENCES

- [1] D. S. Jin, M. R. Matthews, J. R. Ensher, C. E. Wieman, and E. A. Cornell, Phys. Rev. Lett. **78**, 764 (1997).
- [2] D. M. Stamper-Kurn, H. -J. Miesner, S. Inouye, M. R. Andrews, and W. Ketterle, Phys. Rev. Lett. **81**, 500 (1998).
- [3] O. M. Maragò, G. Hechenblaikner, E. Hodby, and C. J. Foot, Phys. Rev. Lett. **86**, 3938 (2001).
- [4] F. Chevy, V. Bretin, P. Rosenbusch, K. W. Madison, and J. Dalibard, Phys. Rev. Lett. **88**, 250402 (2002).
- [5] D. A. W. Hutchinson, E. Zaremba, and A. Griffin, Phys. Rev. Lett. **78**, 1842 (1997).
- [6] R. J. Dodd, M. Edwards, C. W. Clark, and K. Burnett, Phys. Rev. A **57**, R32 (1998).
- [7] D. A. W. Hutchinson, R. J. Dodd, and K. Burnett, Phys. Rev. Lett. **81**, 2198 (1998).
- [8] S. A. Morgan, J. Phys. B **33**, 3847 (2000).
- [9] M. Rusch, S. A. Morgan, D. A. W. Hutchinson, and K. Burnett, Phys. Rev. Lett. **85**, 4844 (2000).
- [10] S. Giorgini, Phys. Rev. A **61**, 063615 (2000).
- [11] M. Guilleumas and L. P. Pitaevskii, Phys. Rev. A **61**, 013602 (2000).
- [12] J. Reidl, A. Csordás, R. Graham, and P. Szépfalussy, Phys. Rev. A **61**, 043606 (2000).
- [13] H. T. C. Stoof, J. Low Temp. Phys. **114**, 11 (1999).
- [14] C. W. Gardiner and P. Zoller, Phys. Rev. A **61**, 033601 (2000), and references therein.
- [15] R. Walser, J. Williams, J. Cooper, and M. Holland, Phys. Rev. A **59**, 3878 (1999).
- [16] E. Zaremba, T. Nikuni, and A. Griffin, J. Low Temp. Phys. **116**, 277 (1999).
- [17] A. Sinatra, C. Lobo, and Y. Castin, Phys. Rev. Lett. **87**, 210404 (2001); cond-mat/0201217.
- [18] M. J. Davis, S. A. Morgan, and K. Burnett, Phys. Rev. Lett. **87**, 160402 (2001); cond-mat/0201571.
- [19] B. Jackson and E. Zaremba, Phys. Rev. A (to be published) [cond-mat/0205421].
- [20] B. Jackson and E. Zaremba, Phys. Rev. Lett. **87**, 100404 (2001).
- [21] B. Jackson and E. Zaremba, Phys. Rev. Lett. **88**, 180402 (2002).
- [22] B. Jackson and E. Zaremba, Phys. Rev. Lett. (to be published) [cond-mat/0206582].
- [23] S. Stringari, Phys. Rev. Lett. **77**, 2360 (1996).
- [24] M. O. da C. Pires and E. J. V. de Passos, J. Phys. B **33**, 3939 (2000).
- [25] Yu. Kagan, E. L. Surkov, and G. V. Shlyapnikov, Phys. Rev. A **54**, R1753 (1996).
- [26] L. P. Pitaevskii and A. Rosch, Phys. Rev. A **55**, R853 (1997).
- [27] D. Guéry-Odelin, F. Zambelli, J. Dalibard, and S. Stringari, Phys. Rev. A **60**, 4851 (1999).
- [28] A. Griffin, W.-C. Wu, and S. Stringari, Phys. Rev. Lett. **78**, 1838 (1997).
- [29] M. Guilleumas and L. P. Pitaevskii, cond-mat/0208047.
- [30] P. O. Fedichev and G. V. Shlyapnikov, Phys. Rev. A **63**, 045601 (2001)

FIGURES

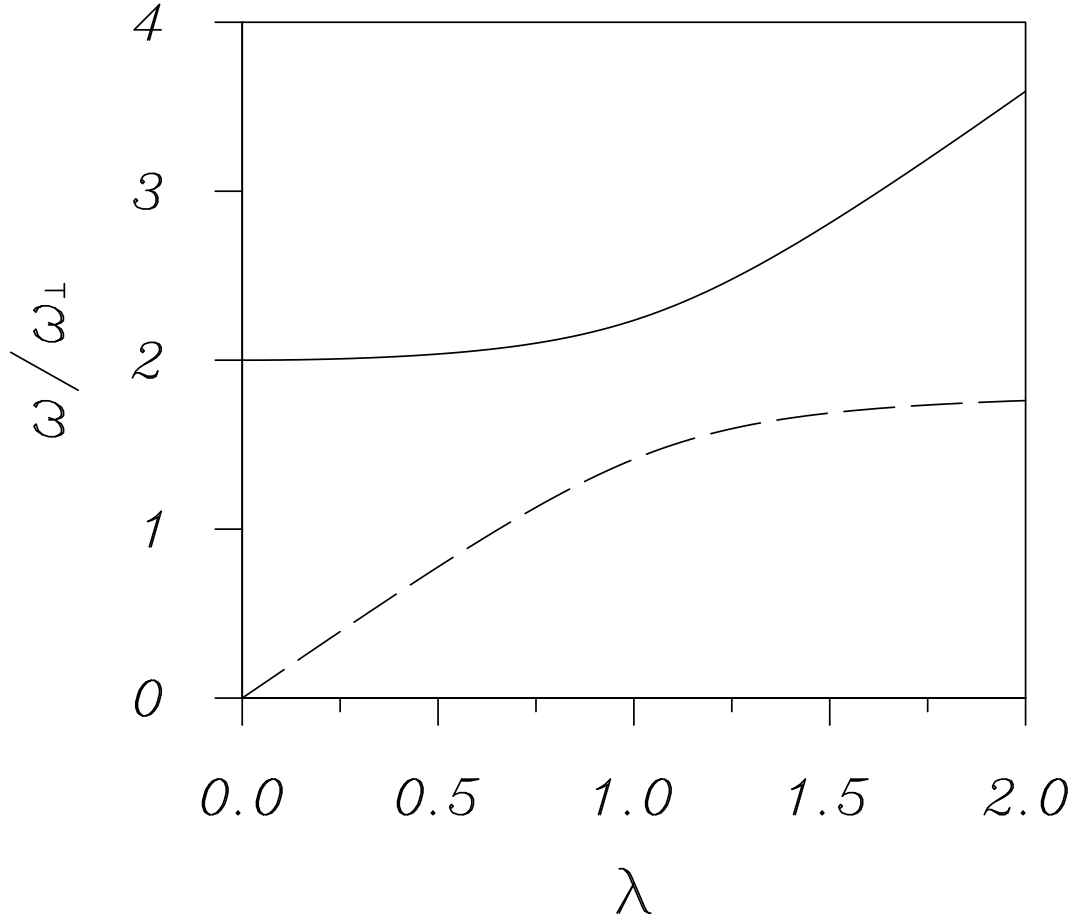


FIG. 1. Frequencies of the lowest $m = 0$ condensate modes in the Thomas-Fermi limit, given by (7), as a function of the anisotropy parameter $\lambda = \omega_z/\omega_\perp$. The higher mode ω_+ (which corresponds to the transverse breathing mode in the $\lambda \rightarrow 0$ limit) is labelled by the solid line, while ω_- is denoted with the dashed line.

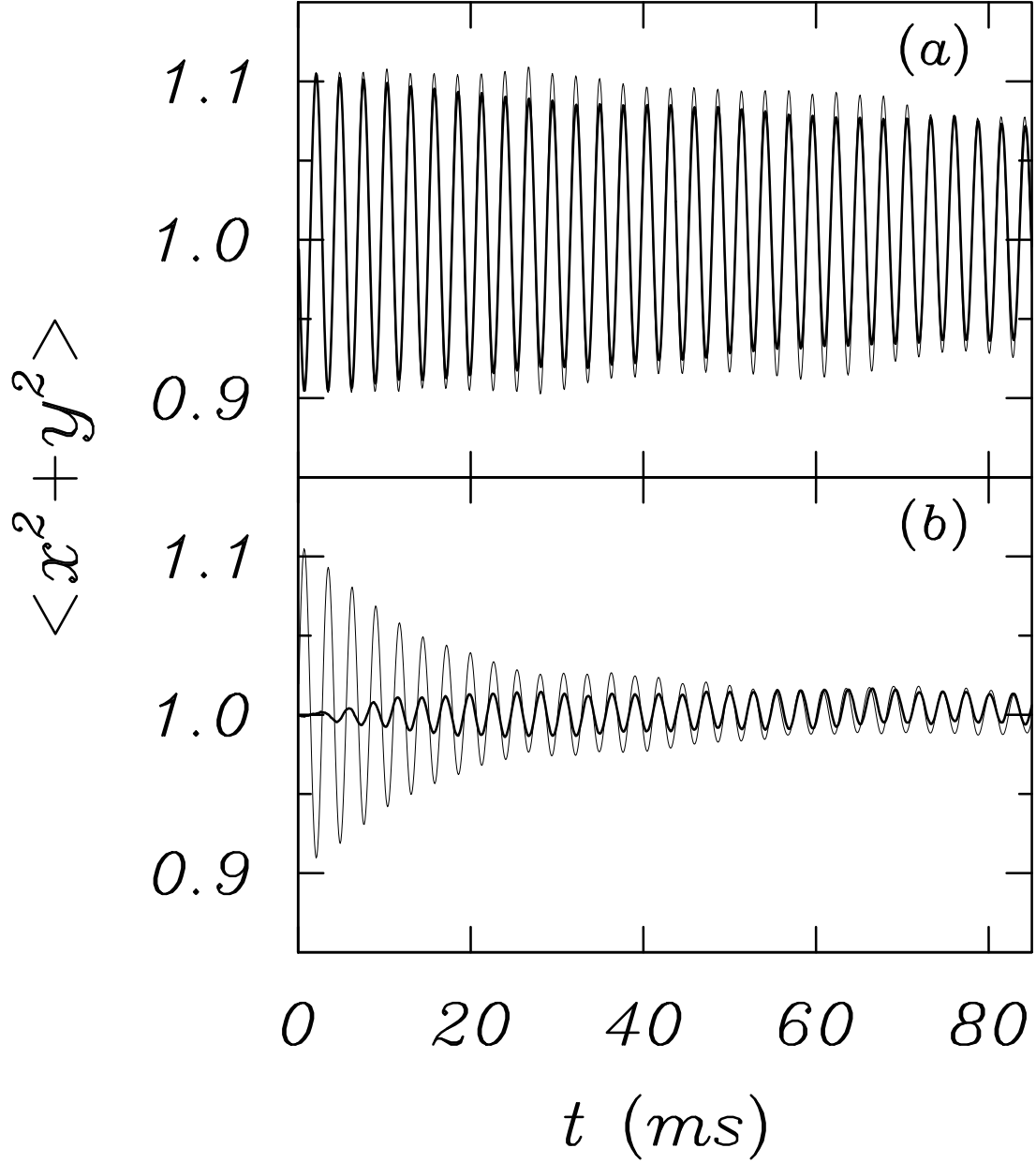


FIG. 2. Time-dependent radial moments for the condensate, χ_c (narrow line) and thermal cloud, χ_n (bold line), divided by the corresponding values at $t = 0$. The figures are for a temperature of $T = 125$ nK, and show the result of (a) exciting the system using the “tophat” perturbation scheme employed experimentally (16), and (b) exciting the condensate only by initially imposing a velocity field of the form $\mathbf{v}_c \propto x\hat{\mathbf{i}} + y\hat{\mathbf{j}}$.

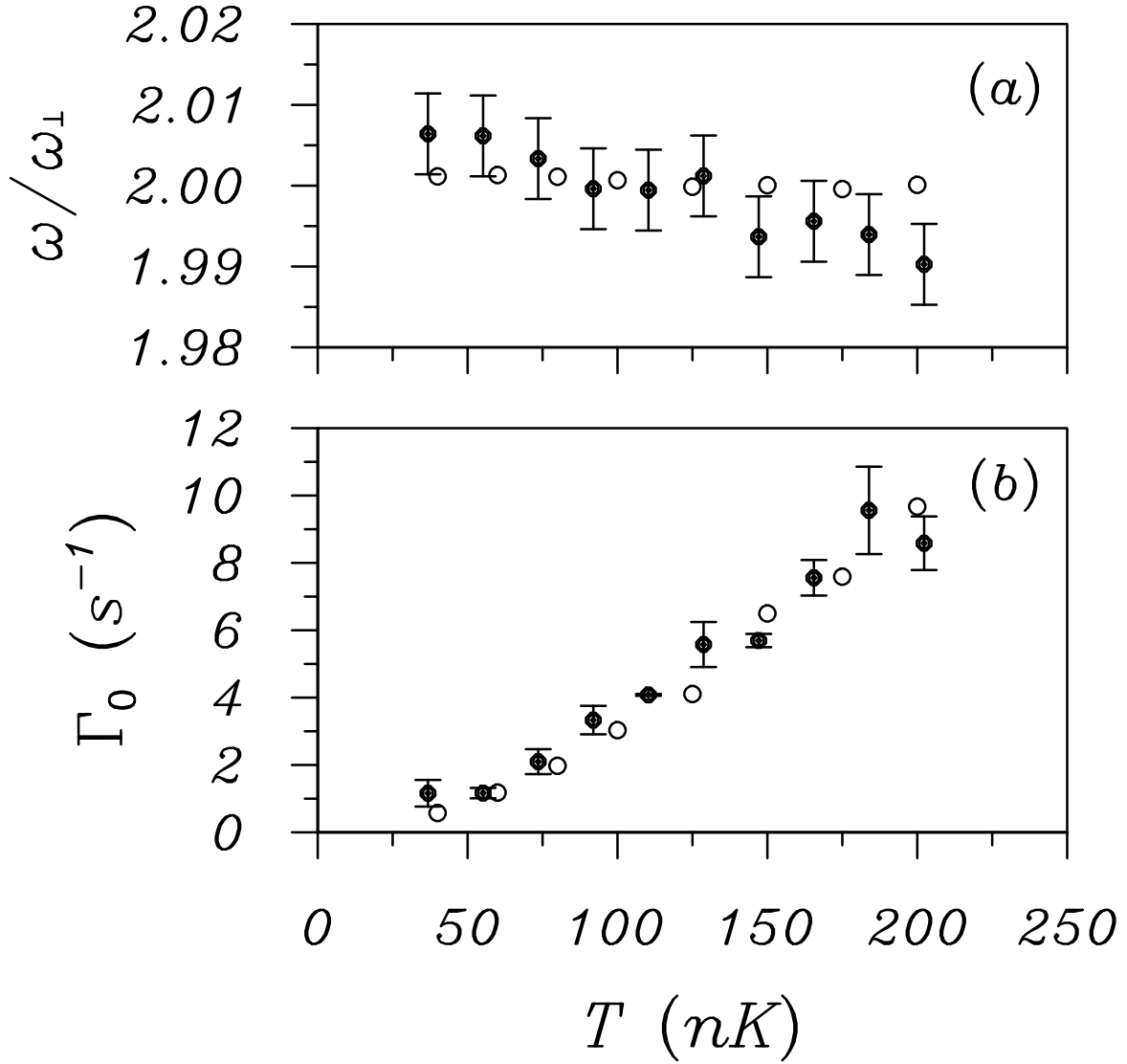


FIG. 3. Frequency (a) and damping rate (b) of the condensate transverse breathing mode. Our results (open circles) are compared to the experimental data of [4] (solid circles), where the simulation parameters and excitation scheme are chosen to match the conditions of the experiment.

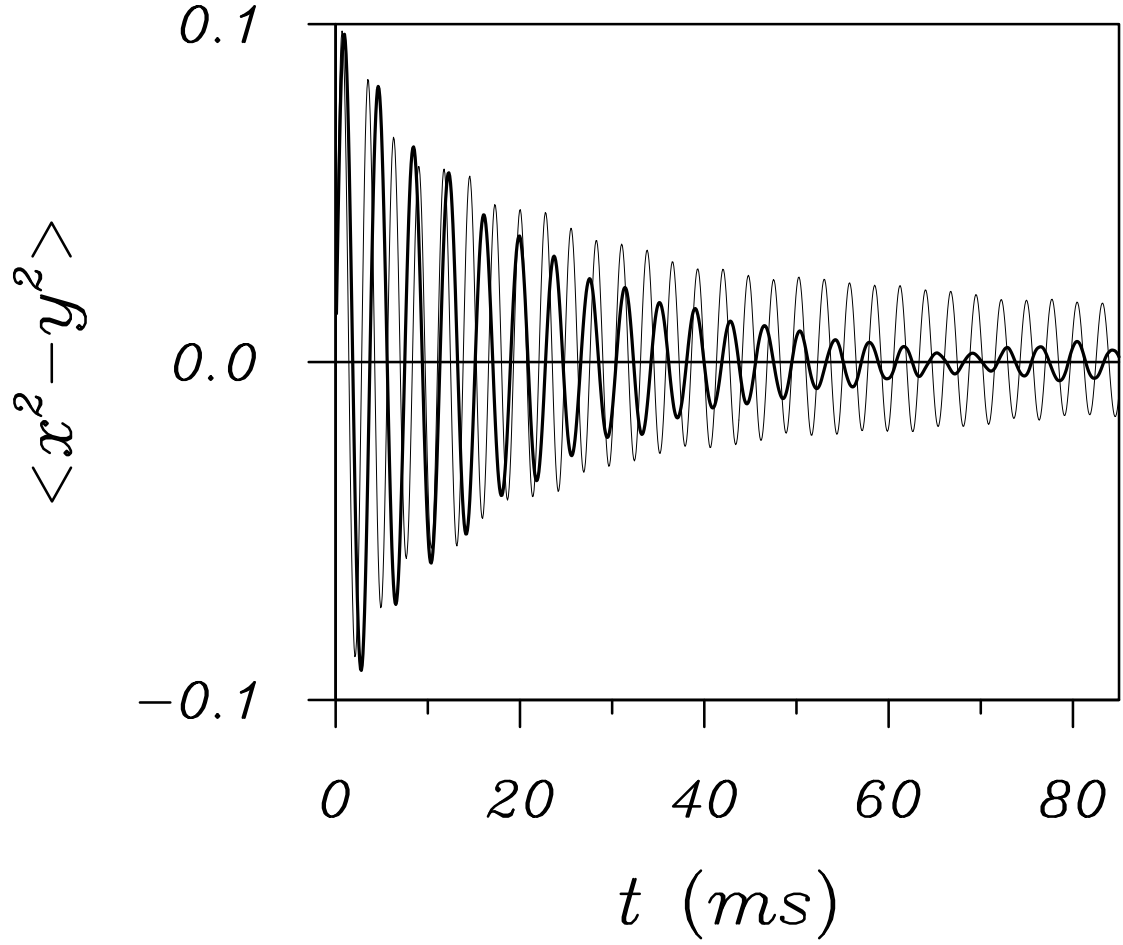


FIG. 4. Time-dependent quadrupole moments $\langle x^2 - y^2 \rangle$ for the condensate (bold line) and thermal cloud (narrow line), where the moments have been scaled so that they overlay one another. The plots are for a temperature of $T = 125$ nK, and show the result of initially imposing a velocity field of the form $\mathbf{v}_{\{c,n\}} \propto x\hat{\mathbf{i}} - y\hat{\mathbf{j}}$ on both components.

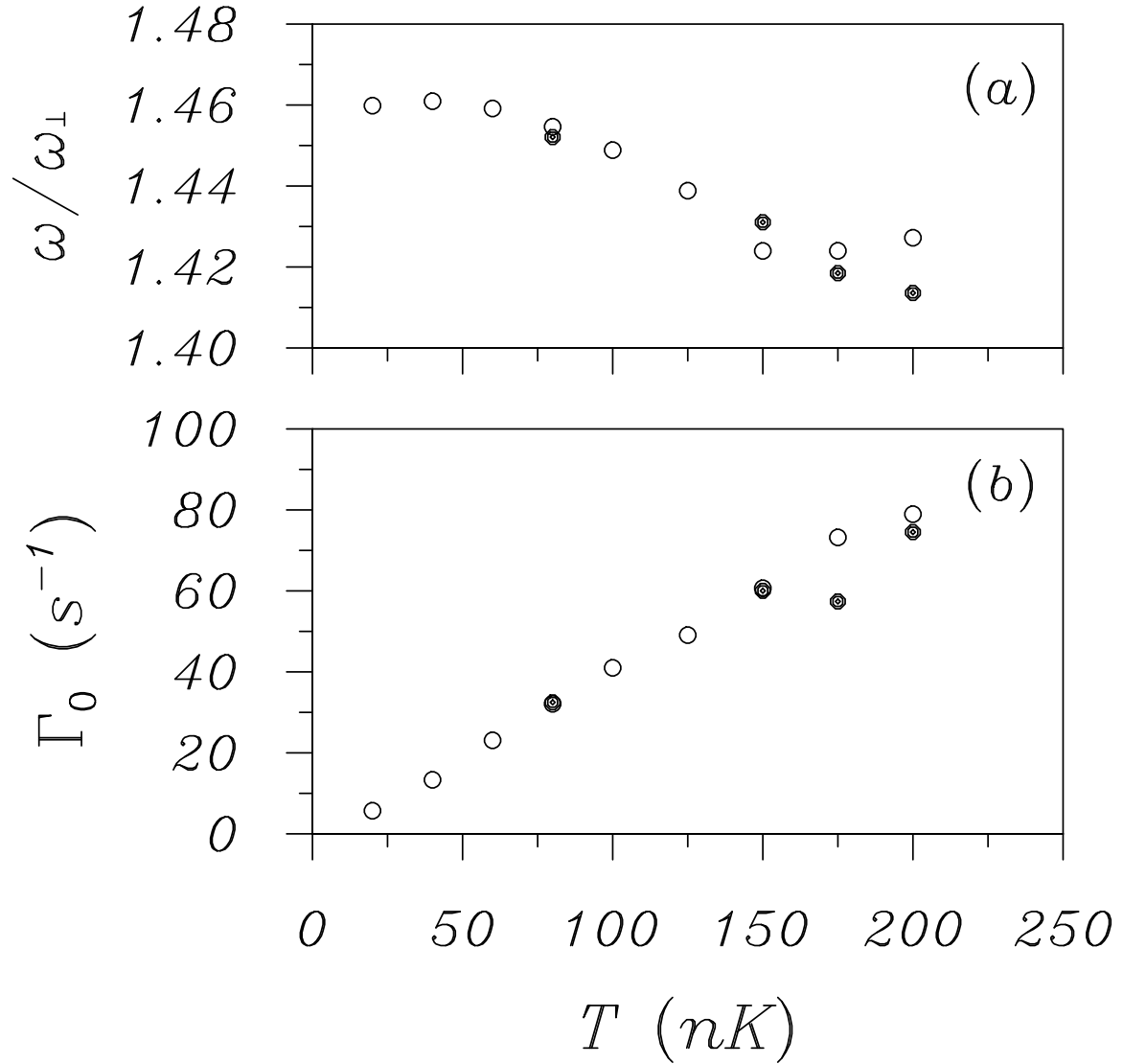


FIG. 5. Frequency (a) and damping rate (b) of the condensate transverse quadrupole mode, where we show the results of initially exciting both components (open circles) and the condensate only (bullets) by imposing a velocity field. Simulation parameters are the same as in Fig. 3.

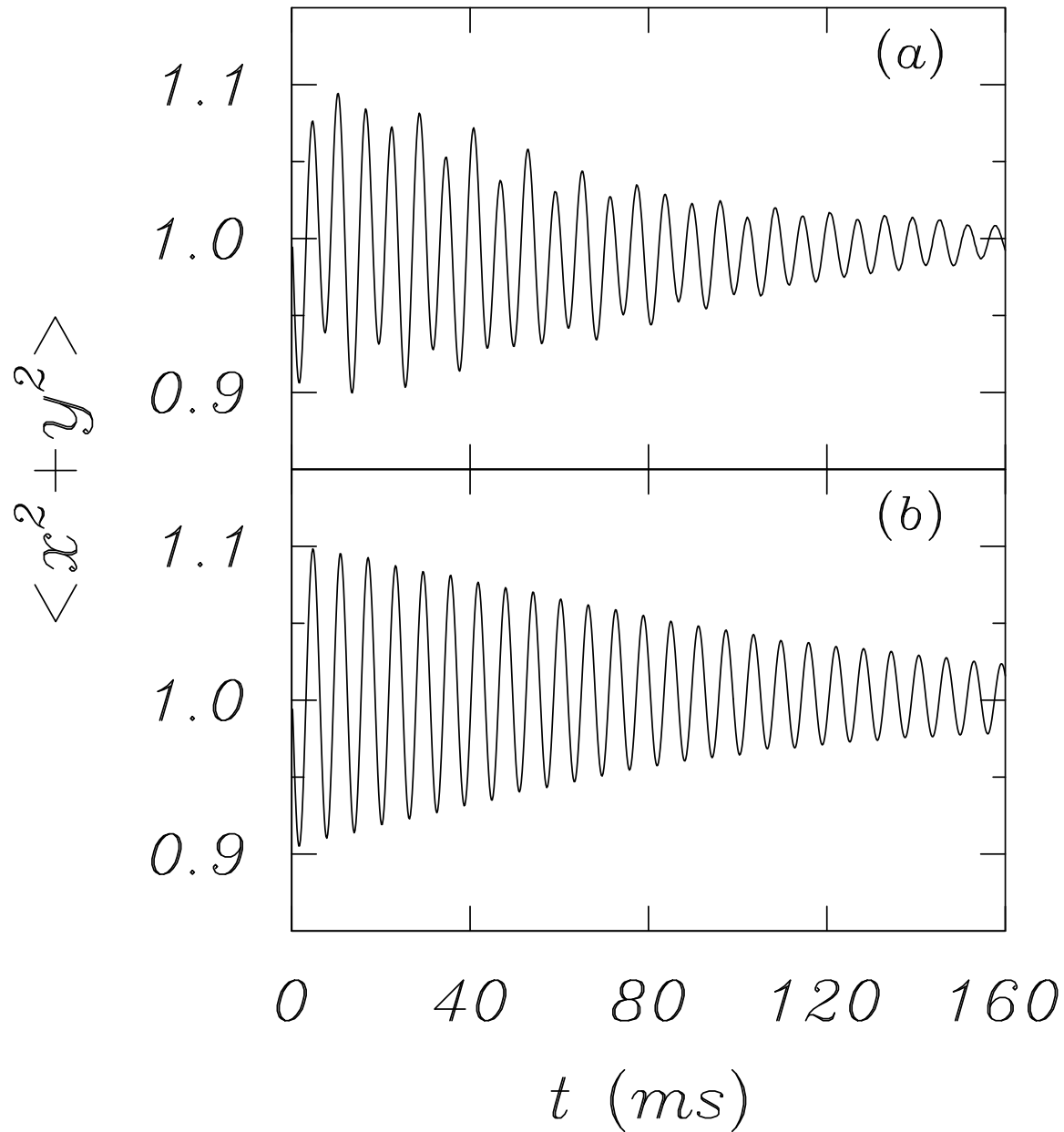


FIG. 6. Time-dependent radial moments for (a) the condensate and (b) the thermal cloud, divided by the corresponding values at $t = 0$, for a less anisotropic trap. The figures are for a temperature of $T = 125$ nK, and show the result of perturbing the system using the stepped excitation in (16). The trap parameters are $\lambda = 0.75$ and $\bar{\omega} = 2\pi \times 73.3$ Hz.